Impact of Pore Size and Surface Chemistry of Porous Silicon Particles and Structure of Phospholipids on Their Interactions

Dongfei Liu,*[†,‡,§] Katriina Lipponen,[†,‡] Peng Quan,[†,‡,⊥] Xiaocao Wan,[⊥] Hongbo Zhang,[‡,∥] Ermei Mäkilä,[#] Jarno Salonen,[#] Risto Kostiainen,[‡] Jouni Hirvonen,[‡] Tapio Kotiaho,[‡,▽] and Hélder A. Santos*[‡,§]

[‡]Drug Research Program, Division of Pharmaceutical Chemistry and Technology, Faculty of Pharmacy, [§]Helsinki Institute of Life Science, HiLIFE, and [▽]Department of Chemistry, Faculty of Science, University of Helsinki, Helsinki FI-00014, Finland

[⊥]Department of Pharmaceutical Science, School of Pharmacy, Shenyang Pharmaceutical University, 103 Wenhua Road, Shenyang, Liaoning 110016, China

[∥]Department of Pharmaceutical Science, Åbo Akademi University, Turku FI-20520, Finland

[#]Laboratory of Industrial Physics, Department of Physics and Astronomy, University of Turku, Turku FI-20014, Finland

S *Supporting Information*

ABSTRACT: By exploiting its porous structure and high loading capacity, porous silicon (PSi) is a promising biomaterial to fabricate protocells and biomimetic reactors. Here, we have evaluated the impact of physicochemical properties of PSi particles [thermally oxidized PSi, TOPSi; annealed TOPSi, AnnTOPSi; (3-aminopropyl) triethoxysilane functionalized thermally carbonized PSi, APTES-TCPSi; and thermally hydrocarbonized PSi, THCPSi] on their surface interactions with different phospholipids. All of the four phospholipids were similarly adsorbed by the surface of PSi particles, except for TOPSi. Among four PSi particles, TOPSi with hydrophilic surface and smaller pore size showed the weakest adsorption toward phosphatidylcholines. By increasing the pore size from roughly 12.5 to 18.0 nm (TOPSi vs AnnTOPSi), the quantity of phosphatidylcholines adsorbed by TOPSi was enhanced to the same level of hydrophilic APTES-TCPSi and hydrophobic THCPSi. The 1,2-dioleoyl-*sn*-glycero-3-phosphocholine (DOPC) exhibited the highest release ratio of phospholipids from all four PSi particles, and phosphatidylserine (DPPS) showed the lowest release ratio of phospholipids from PSi particles, except for TOPSi, which adsorbed less phospholipids due to the small pore size. There is consistency in the release extent of phospholipids from PSi particles and the isosteric heat of adsorption. Overall, our study demonstrates the importance of pore size and surface chemistry of PSi particles as well as the structure of phospholipids on their interactions. The obtained information can be employed to guide the selection of PSi particles and phospholipids to fabricate highly ordered structures, for example, protocells, or biomimetic reactors.

KEYWORDS: *porous silicon, phospholipids, adsorption, surface chemistry, pore size*
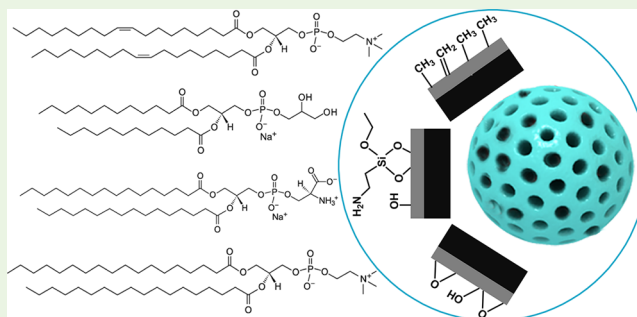
A protocell is defined as a large ordered structure enclosed by a membrane that carries out some life activities. Brinker et al.[1] fabricated a protocell, which was composed of a porous particle-supported lipid bilayer. This protocell synergistically combined the properties of liposomes and porous inorganic particles for targeted delivery of a drug cocktail to cancer cells. The unique features of porous silicon (PSi) materials, including the controllable pore size and volume,[2,3] large surface area,[4,5] and versatile surface chemistry,[6,7] broaden their applications in biomedicine.[8−10] Taking advantages of their high loading capacity to therapeutics, our group has prepared PSi-encapsulated polymeric micro-[11,12] and nano-composites[13,14] for controlled delivery a series of drug combinations.

Besides drug delivery, PSi particles have also been encapsulated in cell membrane-derived vesicles.[15] The cell membrane primarily consists of the amphiphilic phospholipids,[16] which regulate the structural framework of the cell membrane by forming a lipid bilayer.[17] The obtained PSi-encapsulated vesicles exhibited immunostimulant features on human cells, promoting the expression of costimulatory signals and the secretion of pro-inflammatory cytokines.[15] Recently, our group has also engineered the PSi particle embedded-cell membrane vesicles (biomimetic reactors).[18] This PSi-encapsulated reactor served as a biocompartment, readily integrating

with cells, and supplementing the cellular functions under oxidative stress. The PSi-encapsulated vesicles were usually prepared by the film extrusion method,[15,18] showing great potential in biomedical applications. However, the interactions between PSi particles and cell membrane materials, such as phospholipids, remains unclear.

Herein, we studied the interactions between the cell membrane phospholipids and the surface of PSi particles, which can guide the selection of materials to fabricate, for example, stable protocells or biomimetic reactors in the future. As cell membrane includes numerous different types of phospholipids, highly specific and sensitive analytical methods are needed. Mass spectrometry provides a powerful tool for the qualitative and quantitative analysis of phospholipid mixtures and determination of phospholipid structures that facilitates the throughout characterization of protocells and biomimetic reactors.[19,20] Therefore, we employed mass spectrometry to quantitatively analyze the interactions (adsorption and release) between phospholipids and the surface of PSi particles. To simplify the quantitative analysis and comparison, we selected four major structural phospholipids in eukaryotic cell membranes (Figure 1a), including phosphatidylcholines (1,2-dioleoyl-*sn*-glycero-3-phosphocholine, DOPC; 1,2-distearoyl-*sn*-glycero-3-phosphocholine, DSPC), phosphatidylserine (1,2-dipalmitoyl-*sn*-glycero-3-phosphoserine sodium salt, DPPS) and phosphatidylglycerol (1,2-dilauroyl-*sn*-glycero-3-phosphorylglycerol sodium salt, DLPG).[21] The surface chemistry and hydrophilicity of the engineered PSi are summarized in Figure 1b, such as thermally oxidized PSi (TOPSi/AnnTOPSi; hydrophilic),[22,23] (3-aminopropyl)triethoxysilane functionalized thermally carbonized PSi (APTES-TCPSi; hydrophilic)[13,24,25] and thermally hydrocarbonized PSi (THCPSi; hydrophobic).[11,14,26] The average pore size was around 18.1, 12.7, 15.5, and 14.5 nm for AnnTOPSi, TOPSi, APTES-TCPSi and THCPSi (Figure 1c), respectively. The pore volume of the PSi particles was varied from 0.15 to 1.16 cm^3/g (Figure 1d), and the specific surface area was between 34 and 320 cm^2/g (Figure 1e). To study the effect of the pore size and volume on the interactions between PSi particles and phospholipids, annealed TOPSi (AnnTOPSi)[26,27] were used with a larger pore size (approximately 18 nm), lower pore volume (roughly 0.15 cm^3/g), and consequently smaller specific surface area (around 34 cm^2/g), in comparison to TOPSi particles. To reveal the effect of surface chemistry of PSi particles on adsorption and release of phospholipids, the interaction between the surface of PSi particles and phospholipids were studied using configurational bias-Monte Carlo (CBMC) simulations.

First of all, we studied the surface morphology of PSi particles by scanning electron microscopy (SEM) imaging (Figure 2) before and after the incubation with the mixture of four phospholipids (DOPC, DSPC, DPPS and DLPG). The final concentration for each phospholipid was 30 nM in the incubation solution. The average pore size of AnnTOPSi particles (roughly 18.0 nm; Figure 1c) was larger than that of TOPSi (approximately 12.5 nm; Figure 1c), thus the surface morphology change for AnnTOPSi particles was easier to be detected. Therefore, we evaluated the morphology change of AnnTOPSi instead of TOPSi before and after the phospholipids incubation. All three bare PSi particles, AnnTOPSi, THCPSi, and APTES-TCPSi, presented an irregular shape and high surface roughness (Figure 2). Moreover, AnnTOPSi showed smoother surface than the other two PSi particles.
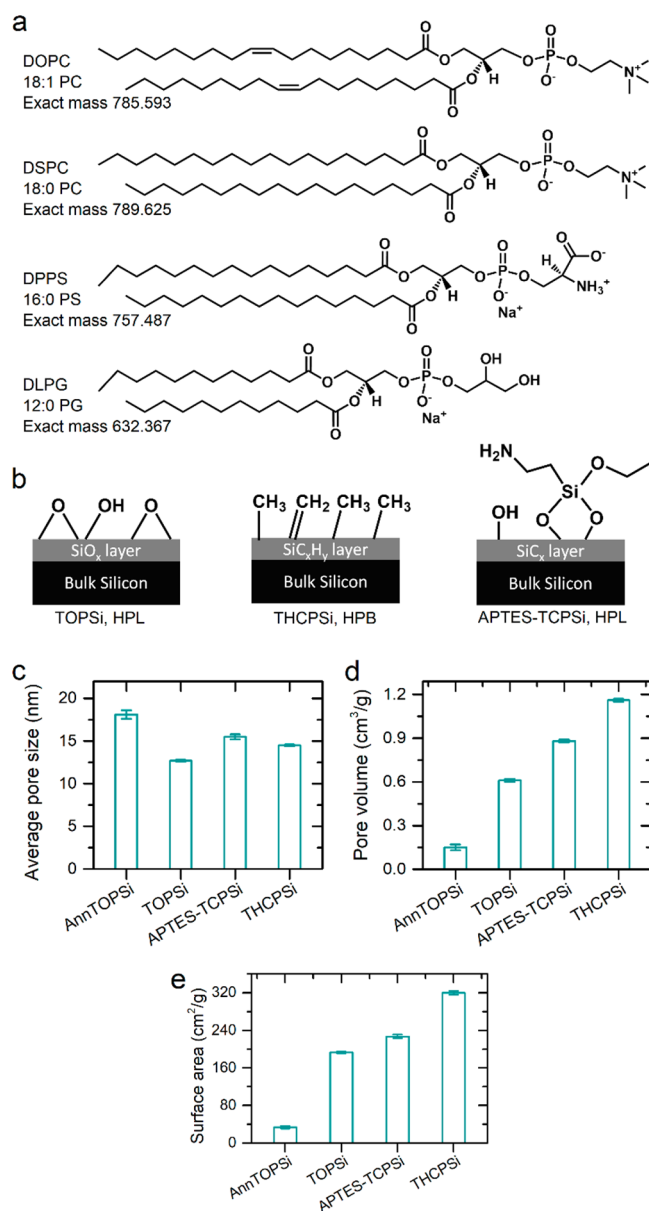

Figure 1. Selected phospholipids and PSi particles. (a) Molecular structure and exact mass of the selected phospholipids, including phosphatidylcholines (DOPC and DSPC), phosphatidylserine (DPPS), and phosphatidylglycerol (DLPG). (b) Surface chemistry and hydrophilicity of the selected PSi particles. HPL, hydrophilic; HPB, hydrophobic. (c−e) Physicochemical properties of PSi particles (*n* = 2), such as (c) pore size, (d) pore volume, and (e) specific surface area.

After incubation with the phospholipids, the pores of PSi particles were at least partially sealed, even for the AnnTOPSi with the largest pore size. Clear morphological change was observed for APTES-TCPSi and AnnTOPSi. Occasionally, we also found PSi particles spherical in shape and fully covered with phospholipids, indicating the potential of PSi particles for the preparation of, for example, protocell based structures[1] (Figure S1). Overall, the SEM images confirmed the adsorption of phospholipids onto the surface of PSi particles.

The absolute amount (the moles) of phospholipid adsorbed onto the surface of PSi particles is summarized in Figure 3. With the concentration growth of phospholipids from 200 to 1000 nM, the level of phospholipids adsorbed onto the surface
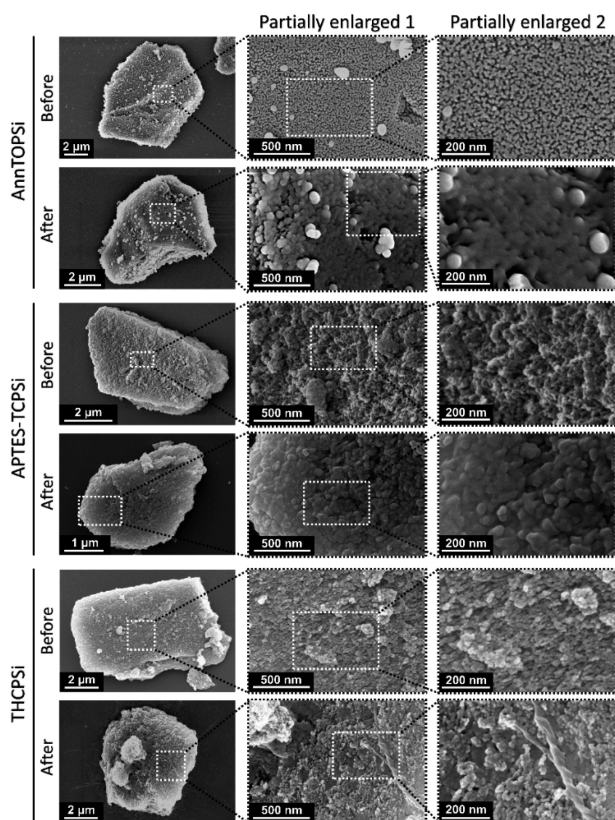
Figure 2. Representative SEM images of PSi particles before and after phospholipid adsorption. PSi particles were incubated with the mixture of four phospholipids, DOPC, DSPC, DPPS, and DLPG; the concentration for each phospholipid was 30 nM. The partially enlarged view of the PSi particles shows clearly that the pores are, at least, partially covered by phospholipids.
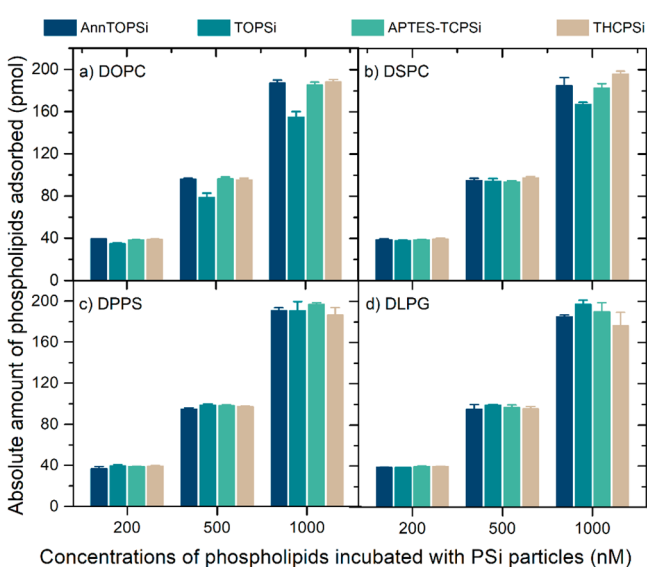

Figure 3. The absolute amount of phospholipid adsorbed onto the surface of PSi particles. The effect of types of phospholipids, (a) DOPC, (b) DSPC, (c) DPPS and (d) DLPG, were tested at room temperature. On the basis of 1 mg of PSi particles, we calculated the amount of phospholipid adsorbed by AnnTOPSi, TOPSi, APTES-TCPSi, and THCPSi. Data are presented as mean ± s.d. (n = 3).

of PSi particles (1 mg) continually increased. Specifically, the adsorption level grew from about 35 to 200 pmol for DOPC,

DSPC, DPPS and DLPG (Figure 3a−d). All four phospholipids achieved a similar adsorption level, which is in accordance to the percentage of phospholipids adsorbed onto the surface of PSi particles (Figure S2). Regardless of the concentrations and types of phospholipids incubated, the percentage of phospholipids adsorbed onto the surface of PSi particles was >90% for all the PSi particles tested, except for TOPSi. The relatively high adsorption of phospholipid can also be ascribed to the local topography of PSi particles. In comparison to the planar surface, Losada-Pérez et al. have showed that the (locally) larger surface area of nanoporous materials results in increased interactions with phospholipids.[28]

Among the selected PSi particles, their difference in pore volume and surface area is much larger than that of pore size. However, the amount of phospholipid adsorbed onto PSi particles were quite close to each other. The phospholipid adsorption data indicated that pore volume and surface area of PSi particles were not the main factor to determine the amount of phospholipid adsorbed. Because of the relative large size of phospholipids (roughly 2.3 nm),[29] the increase in pore size might be in favor of the adsorption of phospholipids onto the surface of PSi particles. By increasing the pore size from around 12.5 to 18.0 nm (TOPSi vs AnnTOPSi), the adsorption of DOPC (500 and 1000 nM) and DSPC (1000 nM) onto the surface of AnnTOPSi was enhanced to the same level of APTES-TCPSi and THCPSi. In contrast, the increase of pore size led to the decrease of surface area from approximately 193 to 34 cm^2/g (TOPSi vs AnnTOPSi). The adsorption of DOPC and DSPC was increased by enlarging the pore size of TOPSi and simultaneously reduced surface area, indicating that not all surface area of TOPSi was contributed to the DOPC and DSPC adsorption. The small pore size impeded the entrance of DOPC and DSPC into the TOPSi particles, and most of the phospholipids may just adsorb on the outside surface of TOPSi particles.

Besides the phospholipid adsorption, we also tested the release of the adsorbed phospholipids from PSi particles (Figure 4 and Figure S3). By comparing the absolute amount of phospholipid adsorbed and released, the absolute amount of phospholipid remained at the surface of PSi particles after the release study have been summarized in Figure S4. Regardless of PSi particles and phospholipids studied, the larger the amount of phospholipid adsorbed by PSi particles, the higher the amount of phospholipid released from the surface of PSi particles. Among all four phospholipids, DOPC showed the highest extent of release from PSi particles, indicating the weakest interaction between DOPC and the surface of PSi particles. Toward PSi particles incubated with DOPC, the level of DOPC release varied from around 30 to 140 pmol (64−100% released), depending on the physicochemical properties of PSi particles and the concentration of phospholipids incubated with PSi particles (Figure 4a). The corresponding amount of phospholipid released from PSi particles decreased to approximately 20 to 140 pmol (48−93% released) for DSPC (Figure 4b), around 4 to 80 pmol (10−58% released) for DPPS (Figure 4c), and roughly 5 to 90 pmol (16−67% released) for DLPG (Figure 4d). The results indicated that DPPS had the strongest interaction with the surface of the PSi particles, and DOPC had the weakest interaction with the surface of the PSi particles.

When looking at the effect of the types of PSi particles on the release of phospholipids, we cannot find a general trend for all four phospholipids tested. In the case of DSPC, the extent
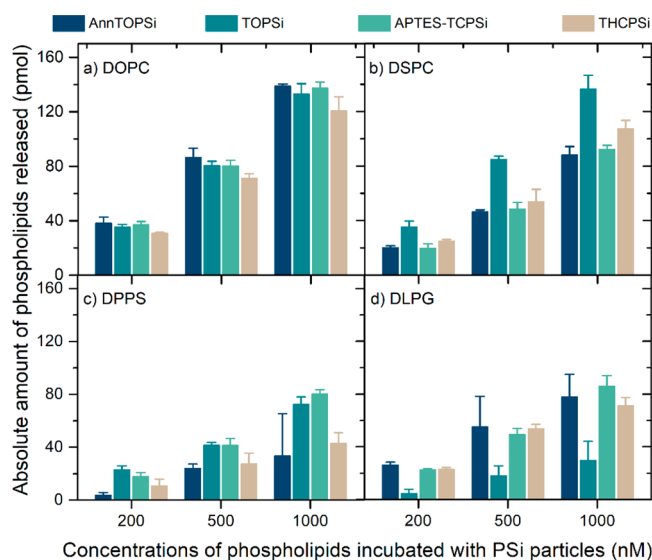
Figure 4. Absolute amount of phospholipid released from the surface of PSi particles. Four phospholipids, (a) DOPC, (b) DSPC, (c) DPPS, and (d) DLPG, were released from the surface of the PSi particles at room temperature. With regard to the absolute amount of phospholipid released, it was calculated based on 1 mg of PSi particles for each, including AnnTOPSi, TOPSi, APTES-TCPSi, and THCPSi. Data are presented as mean ± s.d. ($n = 3$).

Figure 5. Isosteric heat of adsorption (Q_{st}) calculated with different phospholipids and PSi particles. (a) DOPC, (b) DSPC, (c) DPPS, and (d) DLPG. DPPS showed the highest isosteric heat of adsorption among the four phospholipids, which indicated the strongest interaction between DPPS and the surface of PSi particles.

of phospholipid released from TOPSi was higher than that of the other three PSi particles at all three DSPC concentration levels. In comparison to DSPC, an opposite trend was observed on the level of DLPG released from TOPSi particles. Only around 30 pmol DLPG was released from the surface of TOPSi particles, for which approximately 200 pmol DLPG was adsorbed when incubated with a DLPG concentration of 1000 nM. These results indicated that both the pore size of the PSi particles and the physicochemical properties of the phospholipids had an effect on the interaction between the PSi particles and the phospholipids.

Besides the pore size of PSi particles, the surface hydrophobicity[30] and functional groups[31,32] may play an important role in phospholipid adsorption.[28] The isosteric heat of adsorption (Qst, kJ/mol) calculated by the configurational bias-Monte Carlo (CBMC) simulation[33] has been illustrated in Figure 5. Regardless of the types of PSi particles, DPPS showed the strongest interaction with PSi particles among all four phospholipids. The isosteric heat of adsorption results are in good agreement with the amount of phospholipid released from PSi particles (Figure 4), except for TOPSi. This inconsistency for TOPSi can be attributed to its small pore size, because the calculated isosteric heat did not take into account the pore size of PSi particles. The interaction between DPPS and the surface of PSi particles was affected by van der Waals energy and electrostatic energy (Figure S5). Moreover, the contribution of electrostatic energy was higher than that of van der Waals energy. For DOPC and DSPC, van der Waals energy played a more important role on the interaction compare to electrostatic energy. The interaction between DLPG and the surface of PSi particles was mainly affected by van der Waals energy (Figure S5). Among all four PSi particles, THCPSi is the only one with a nonpolar surface. Therefore, the electrostatic attraction of THCPSi toward phospholipid is expected to be the lowest, which is in agreement with the electrostatic energy calculated by CBMC simulation. A
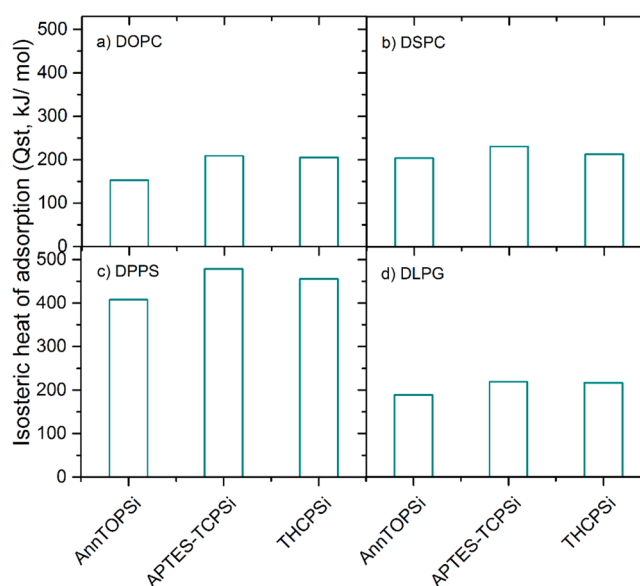
nonpolar surface should always develop attractive van der Waals forces,[34,35] which can explain the strongest van der Waals force between THCPSi and phospholipid among the PSi particles tested.

In conclusion, we have tested the impact of surface hydrophobicity and functional groups, and pore size of PSi particles on the adsorption and release of different phospholipids. The quantitative analysis of phospholipids was achieved by the developed mass spectrometric method. In general, PSi particles, except for TOPSi, adsorbed similar amount of different kinds of phospholipids. Among all four PSi particles studied, TOPSi adsorbed the lowest amount of DOPC and DSPC due to the relative small pore size and large size of the phospholipids. Regarding the types of phospholipids, DPPS showed the strongest interaction with the surface of PSi particles. Already this study can help the selection of PSi particles and phospholipids to fabricate highly ordered structures, for example, stable protocells or biomimetic reactors, for biomedical applications. However, more detailed studies with larger set of solvent systems and lipids are needed to draw precise conclusions about the effect of physicochemical characteristics of phospholipids and PSi particles on their interactions.

■ ASSOCIATED CONTENT

Ⓢ Supporting Information

The Supporting Information is available free of charge on the ACS Publications website at DOI: 10.1021/acsbiomaterials.8b00343.

> Details of the experimental procedures, characterization results of SEM images, relative and absolute percentage of phospholipids adsorbed onto the surface of PSi particles, and absolute amount of phospholipids remained at the surface of PSi particles after the release study (PDF)

■ AUTHOR INFORMATION

Corresponding Authors
*E-mail: dongfei.liu@helsinki.fi (D.L.).
*E-mail: helder.santos@helsinki.fi (H.A.S.).

ORCID ⊙
Dongfei Liu: 0000-0002-2426-134X
Ermei Mäkilä: 0000-0002-8300-6533
Jarno Salonen: 0000-0002-5245-742X
Risto Kostiainen: 0000-0003-2454-4574
Tapio Kotiaho: 0000-0003-0382-8578
Hélder A. Santos: 0000-0001-7850-6309

Author Contributions
[†]D.L., K.L., and P.Q. contributed equally to this work.

Notes
The authors declare no competing financial interest.

■ REFERENCES

(1) Ashley, C. E.; Carnes, E. C.; Phillips, G. K.; Padilla, D.; Durfee, P. N.; Brown, P. A.; Hanna, T. N.; Liu, J.; Phillips, B.; Carter, M. B.; Carroll, N. J.; Jiang, X.; Dunphy, D. R.; Willman, C. L.; Petsev, D. N.; Evans, D. G.; Parikh, A. N.; Chackerian, B.; Wharton, W.; Peabody, D. S.; Brinker, C. J. The Targeted Delivery of Multicomponent Cargos to Cancer Cells by Nanoporous Particle-Supported Lipid Bilayers. *Nat. Mater.* **2011**, *10* (5), 389−97.

(2) Herino, R.; Bomchil, G.; Barla, K.; Bertrand, C.; Ginoux, J. L. Porosity and Pore Size Distributions of Porous Silicon Layers. *J. Electrochem. Soc.* **1987**, *134* (8), 1994−2000.

(3) Anglin, E. J.; Cheng, L. Y.; Freeman, W. R.; Sailor, M. J. Porous Silicon in Drug Delivery Devices and Materials. *Adv. Drug Delivery Rev.* **2008**, *60* (11), 1266−1277.

(4) Björkqvist, M.; Salonen, J.; Paski, J.; Laine, E. Characterization of Thermally Carbonized Porous Silicon Humidity Sensor. *Sens. Actuators, A* **2004**, *112* (2−3), 244−247.

(5) Stewart, M. P.; Buriak, J. M. Chemical and Biological Applications of Porous Silicon Technology. *Adv. Mater.* **2000**, *12* (12), 859−869.

(6) Santos, H. A.; Riikonen, J.; Salonen, J.; Mäkilä, E.; Heikkilä, T.; Laaksonen, T.; Peltonen, L.; Lehto, V. P.; Hirvonen, J. In Vitro Cytotoxicity of Porous Silicon Microparticles: Effect of the Particle Concentration, Surface Chemistry and Size. *Acta Biomater.* **2010**, *6* (7), 2721−2731.

(7) Riikonen, J.; Salomäki, M.; van Wonderen, J.; Kemell, M.; Xu, W.; Korhonen, O.; Ritala, M.; MacMillan, F.; Salonen, J.; Lehto, V. P. Surface Chemistry, Reactivity, and Pore Structure of Porous Silicon Oxidized by Various Methods. *Langmuir* **2012**, *28* (28), 10573−83.

(8) Santos, H. A.; Salonen, J.; Bimbo, L. M.; Lehto, V. P.; Peltonen, L.; Hirvonen, J. Mesoporous Materials as Controlled Drug Delivery Formulations. *J. Drug Delivery Sci. Technol.* **2011**, *21* (2), 139−155.

(9) Santos, H. A.; Mäkilä, E.; Airaksinen, A. J.; Bimbo, L. M.; Hirvonen, J. Porous Silicon Nanoparticles for Nanomedicine: Preparation and Biomedical Applications. *Nanomedicine* **2014**, *9* (4), 535−554.

(10) Santos, H. A.; Bimbo, L. M.; Lehto, V. P.; Airaksinen, A. J.; Salonen, J.; Hirvonen, J. Multifunctional Porous Silicon for Therapeutic Drug Delivery and Imaging. *Curr. Drug Discovery Technol.* **2011**, *8* (3), 228−249.

(11) Liu, D.; Zhang, H.; Herranz-Blanco, B.; Mäkilä, E. M.; Lehto, V. P.; Salonen, J.; Hirvonen, J. T.; Santos, H. A. Microfluidic Assembly of Monodisperse Multistage Ph-Responsive Polymer/ Porous Silicon Composites for Precisely Controlled Multi-Drug Delivery. *Small* **2014**, *10* (10), 2029−2038.

(12) Zhang, H.; Liu, D.; Shahbazi, M. A.; Mäkilä, E. M.; Herranz-Blanco, B.; Salonen, J.; Hirvonen, J. T.; Santos, H. A. Fabrication of a Multifunctional Nano-in-Micro Drug Delivery Platform by Microfluidic Templated Encapsulation of Porous Silicon in Polymer Matrix. *Adv. Mater.* **2014**, *26* (26), 4497−503.

(13) Liu, D.; Zhang, H.; Mäkilä, E. M.; Fan, J.; Herranz-Blanco, B.; Wang, C. F.; Rosa, R.; Ribeiro, A. J.; Salonen, J.; Hirvonen, J. T.; Santos, H. A. Microfluidic Assisted One-Step Fabrication of Porous Silicon@Acetalated Dextran Nanocomposites for Precisely Controlled Combination Chemotherapy. *Biomaterials* **2015**, *39*, 249−59.

(14) Liu, D.; Mäkilä, E. M.; Zhang, H.; Herranz, B.; Kaasalainen, M.; Kinnari, P.; Salonen, J.; Hirvonen, J. T.; Santos, H. A. Nanostructured Porous Silicon-Solid Lipid Nanocomposite: Towards Enhanced Cytocompatibility and Stability, Reduced Cellular Association, and Prolonged Drug Release. *Adv. Funct. Mater.* **2013**, *23* (15), 1893−1902.

(15) Fontana, F.; Shahbazi, M. A.; Liu, D.; Zhang, H.; Mäkilä, E. M.; Salonen, J.; Hirvonen, J. T.; Santos, H. A. Multistaged Nanovaccines Based on Porous Silicon@Acetalated Dextran@Cancer Cell Membrane for Cancer Immunotherapy. *Adv. Mater.* **2017**, *29* (7), 1603239.

(16) Alberts, B.; Johnson, A.; Lewis, J.; Morgan, D.; Raff, M.; Roberts, K.; Walter, P. *Molecular Biology of the Cell*; Garland Science: 2014.

(17) Lingwood, D.; Simons, K. Lipid Rafts as a Membrane-Organizing Principle. *Science* **2010**, *327* (5961), 46−50.

(18) Balasubramanian, V.; Correia, A.; Zhang, H.; Fontana, F.; Mäkilä, E. M.; Salonen, J.; Hirvonen, J. T.; Santos, H. A. Biomimetic Engineering Using Cancer Cell Membranes for Designing Compartmentalized Nanoreactors with Organelle-Like Functions. *Adv. Mater.* **2017**, *29* (11), 1605375.

(19) Wood, P. L. Mass Spectrometry Strategies for Clinical Metabolomics and Lipidomics in Psychiatry, Neurology, and Neuro-Oncology. *Neuropsychopharmacology* **2014**, *39* (1), 24−33.

(20) Han, X. L.; Yang, K.; Gross, R. W. Multi-Dimensional Mass Spectrometry-Based Shotgun Lipidomics and Novel Strategies for Lipidomic Analyses. *Mass Spectrom. Rev.* **2012**, *31* (1), 134−178.

(21) Boesze-Battaglia, K.; Schimmel, R. J. Cell Membrane Lipid Composition and Distribution: Implications for Cell Function and Lessons Learned from Photoreceptors and Platelets. *J. Exp. Biol.* **1997**, *200* (23), 2927−2936.

(22) Salonen, J.; Laitinen, L.; Kaukonen, A. M.; Tuura, J.; Björkqvist, M.; Heikkilä, T.; Vähä-Heikkilä, K.; Hirvonen, J.; Lehto, V. P. Mesoporous Silicon Microparticles for Oral Drug Delivery: Loading and Release of Five Model Drugs. *J. Controlled Release* **2005**, *108* (2−3), 362−74.

(23) Liu, D.; Bimbo, L. M.; Mäkilä, E. M.; Villanova, F.; Kaasalainen, M.; Herranz-Blanco, B.; Caramella, C. M.; Lehto, V. P.; Salonen, J.; Herzig, K. H.; Hirvonen, J. T.; Santos, H. A. Co-Delivery of a Hydrophobic Small Molecule and a Hydrophilic Peptide by Porous Silicon Nanoparticles. *J. Controlled Release* **2013**, *170* (2), 268−78.

(24) Wang, C. F.; Mäkilä, E. M.; Kaasalainen, M. H.; Liu, D.; Sarparanta, M. P.; Airaksinen, A. J.; Salonen, J. J.; Hirvonen, J. T.; Santos, H. A. Copper-Free Azide-Alkyne Cycloaddition of Targeting Peptides to Porous Silicon Nanoparticles for Intracellular Drug Uptake. *Biomaterials* **2014**, *35* (4), 1257−66.

(25) Mäkilä, E.; Bimbo, L. M.; Kaasalainen, M.; Herranz, B.; Airaksinen, A. J.; Heinonen, M.; Kukk, E.; Hirvonen, J.; Santos, H. A.; Salonen, J. Amine Modification of Thermally Carbonized Porous Silicon with Silane Coupling Chemistry. *Langmuir* **2012**, *28* (39), 14045−54.

(26) Limnell, T.; Riikonen, J.; Salonen, J.; Kaukonen, A. M.; Laitinen, L.; Hirvonen, J.; Lehto, V. P. Surface Chemistry and Pore Size Affect Carrier Properties of Mesoporous Silicon Microparticles. *Int. J. Pharm.* **2007**, *343* (1−2), 141−147.

(27) Salonen, J.; Mäkilä, E.; Riikonen, J.; Heikkilä, T.; Lehto, V. P. Controlled Enlargement of Pores by Annealing of Porous Silicon. *Phys. Status Solidi A* **2009**, *206* (6), 1313−1317.

(28) Losada-Perez, P.; Polat, O.; Parikh, A. N.; Seker, E.; Renner, F. U. Engineering the Interface between Lipid Membranes and Nanoporous Gold: A Study by Quartz Crystal Microbalance with Dissipation Monitoring. *Biointerphases* **2018**, *13* (1), 011002.

(29) Kucerka, N.; Tristram-Nagle, S.; Nagle, J. F. Closer Look at Structure of Fully Hydrated Fluid Phase Dppc Bilayers. *Biophys. J.* **2006**, *90* (11), L83−L85.

(30) Tero, R.; Watanabe, H.; Urisu, T. Supported Phospholipid Bilayer Formation on Hydrophilicity-Controlled Silicon Dioxide Surfaces. *Phys. Chem. Chem. Phys.* **2006**, *8* (33), 3885−3894.

(31) Cha, T.; Guo, A.; Zhu, X. Y. Formation of Supported Phospholipid Bilayers on Molecular Surfaces: Role of Surface Charge Density and Electrostatic Interaction. *Biophys. J.* **2006**, *90* (4), 1270−1274.

(32) Kim, Y. H.; Rahman, M. M.; Zhang, Z. L.; Misawa, N.; Tero, R.; Urisu, T. Supported Lipid Bilayer Formation by the Giant Vesicle Fusion Induced by Vesicle-Surface Electrostatic Attractive Interaction. *Chem. Phys. Lett.* **2006**, *420* (4−6), 569−573.

(33) Torres, P.; Bojanich, L.; Sanchez-Varretti, F.; Ramirez-Pastor, A. J.; Quiroga, E.; Boeris, V.; Narambuena, C. F. Protonation of Beta-Lactoglobulin in the Presence of Strong Polyelectrolyte Chains: A Study Using Monte Carlo Simulation. *Colloids Surf., B* **2017**, *160*, 161−168.

(34) Leonenko, Z. V.; Finot, E.; Ma, H.; Dahms, T. E. S.; Cramb, D. T. Investigation of Temperature-Induced Phase Transitions in Dopc and Dppc Phospholipid Bilayers Using Temperature-Controlled Scanning Force Microscopy. *Biophys. J.* **2004**, *86* (6), 3783−3793.

(35) Moerz, S. T.; Huber, P. Protein Adsorption into Mesopores: A Combination of Electrostatic Interaction, Counterion Release, and Van Der Waals Forces. *Langmuir* **2014**, *30* (10), 2729−2737.